

Novel Diamide-Based Inhibitors of IMPDH

Henry H. Gu,* Edwin J. Iwanowicz, Junqing Guo, Scott H. Watterson, Zhongqi Shen, William J. Pitts, T. G. Murali Dhar, Catherine A. Fleener, Katherine Rouleau, N. Z. Sherbina, Mark Witmer, Jeffrey Tredup and Diane Hollenbaugh

Bristol-Myers Squibb Pharmaceutical Research Institute, Princeton, NJ 08543-4000, USA

Received 24 October 2001; accepted 5 February 2002

Abstract—A series of novel amide-based small molecule inhibitors of inosine monophosphate dehydrogenase is described. The synthesis and the structure–activity relationships (SARs) derived from in vitro studies are presented. © 2002 Elsevier Science Ltd. All rights reserved.

Inosine monophosphate dehydrogenase (IMPDH), a key enzyme in the de novo synthesis of guanosine nucleotides, catalyzes the irreversible NAD-dependent oxidation of inosine-5'-monophosphate (IMP) to xanthosine-5'-monophosphate (XMP).¹ Two distinct genes encoding IMPDH have been identified and the gene products are labeled type I and type II. The proteins are of identical size (514 amino acids)^{2–4} and share 84% sequence identity. B- and T-lymphocytes depend on the de novo, rather than the salvage pathway, in the generation of nucleotides. Due to the unique reliance of lymphocytes on the de novo pathway, IMPDH is an attractive target for selectively inhibiting an immune response, without undue inhibition of other proliferating cells.

Mycophenolic acid (MPA, Fig. 1) and some of its derivatives have been shown to be potent, uncompetitive, reversible inhibitors of human IMPDH type I and type II.^{5,6} MPA has been demonstrated to block the response of B- and T-cells to mitogen or antigen. IMPDH inhibitors, such as MPA and the prodrug CellCept[®], are useful therapies in the treatment of transplant rejection and have been found to have effects in autoimmune disorders, such as psoriasis and rheumatoid arthritis.⁷ In addition, various cancer cell lines are sensitive to IMPDH inhibition, and thus clinical trials evaluating IMPDH inhibitors for their antileukemic effects have been undertaken.⁸

Dose-limiting gastrointestinal (GI) toxicity is observed from oral administration of either MPA or CellCept[®] in a clinical setting. Seminal contributions by Vertex have shown that biarylureas, exemplified by VX-497, are highly potent inhibitors of IMPDH catalytic activity (Fig. 1).⁹ This compound is currently under evaluation in the clinic and is expected to have an improved therapeutic window with regard to GI toxicity-limiting dosing.

Our focus is the identification and development of potent, selective inhibitors of IMPDH with improved physical and pharmacological properties and fewer side effects. In this report, we outline the synthesis and

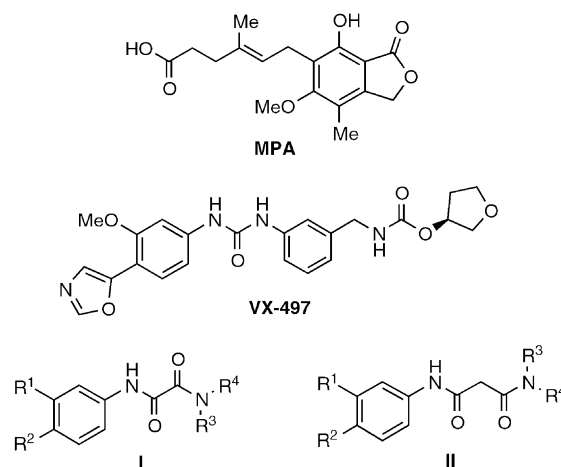


Figure 1. Chemical structures of MPA, VX-497, and diamides I and II.

*Corresponding author. Fax: +1-609-252-6601; e-mail: henry.gu@bms.com

biological evaluation of a new class of inhibitors of IMPDH, based on the diamide backbones **I** and **II** (Fig. 1).

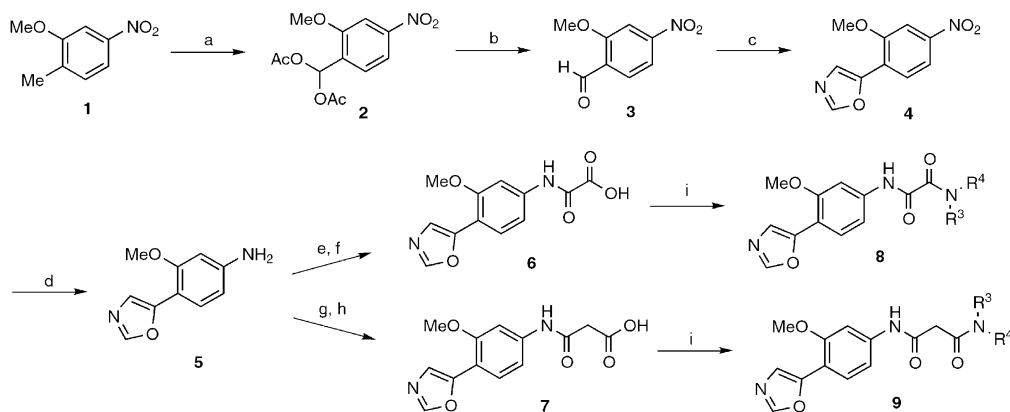
The synthesis of diamide analogues **8** and **9** is shown in Scheme 1. The 3-methoxy-4-(5-oxazolyl)-aniline **5** was prepared from 2-methoxy-4-nitro-toluene **1** on a multi-gram scale utilizing a synthetic procedure described by Vertex.¹⁰ Acylation of **5** with ethyl oxalyl chloride gave the corresponding oxalamic acid ethyl ester, which was hydrolyzed to generate the oxalamic acid **6**. In a similar synthetic sequence, the malonic acid **7** was prepared utilizing ethyl malonyl chloride as the acylating agent. Amides **8** and **9** were synthesized from **6** and **7**, respectively, by treatment with the corresponding amine and utilizing BOP as the coupling agent.¹¹ The syntheses of anilines **12** and **16**, described in Scheme 2, were prepared according to literature procedures.^{10,12} Compound **1c** was prepared from compound **6** utilizing [(3-aminophenyl)methyl] carbamic acid [(3*S*)-tetrahydro-3-furanyl] ester **B** under the standard BOP-coupling conditions.¹³ Compounds **1q** and **1r** were prepared from 4-(5-oxazolyl)-aniline and **12**, respectively, utilizing the reaction sequence for the conversion of **5** to **8**.

The structure–activity relationships for the inhibition of IMPDH type II catalytic activity are summarized in Table 1. In the ethanediamide series **I**, several lipophilic residues were examined in the R³ and R⁴ positions. Compound **1a** (R⁴=Ph) displayed an IC₅₀ value of

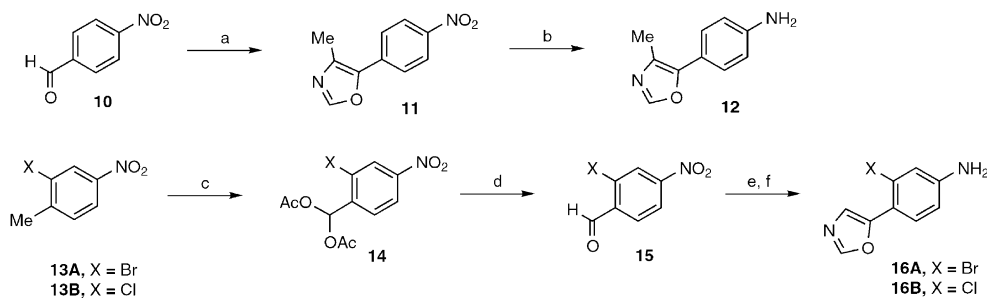
0.052 μM (IMPDH II). With R³ fixed as H, other lipophilic residues were examined at the R⁴ position. Analogues with R⁴ as benzyl **1e**, cyclohexyl **1f**, *n*-propyl **1g**, and *iso*-propyl **1h** were all inactive when tested at the 10 μM concentration. In contrast, the *t*-butyl analogue **1i**, displayed an IC₅₀ of 0.010 μM. Assessment of **1b** and **1j**, both bearing methyl substitution at R³, demonstrated the necessity for substitution with hydrogen to achieve high potency. The R⁴ phenyl of **1a** may be effectively substituted. Compound **1c**, functionalized with a carbamate side chain from VX-497, displayed an IC₅₀ value of 0.030 μM.

In general, analogues where R⁴ has a quaternary center at the site of attachment retain potency. Compound **1o**, featuring a carboxylic acid moiety, is the exception in this group. Notably, when the *gem*-dimethyl residues of R⁴ were fashioned into a cyclopentane ring giving **1l**, potency was maintained. We found that small structural changes to the 3-methoxy-4-(5-oxazolyl)-aniline moiety led to significant changes in potency. Where replacement of the methoxy residue with a bromide (**1s**) or chloride (**1t**) moiety was tolerated, removal of the methoxy residue (**1q**) was not. Similarly, utilizing 4-methyl-5-oxazolyl aniline as a replacement for **5** giving **1r**, led to a significant loss in potency.

Propanediamide analogue **11a** with phenyl as the R⁴ residue displayed potent inhibitory activity against

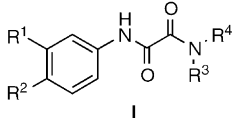


Scheme 1. Reagents and conditions: (a) HOAc, Ac₂O, concd H₂SO₄, CrO₃, 0–10 °C (51%); (b) concd HCl, dioxane, reflux (91%); (c) TosMIC, K₂CO₃, MeOH, reflux (84%); (d) 40 psi H₂, Pd/C, EtOH, (95%); (e) ClCOCOOEt, Et₃N, CH₂Cl₂ (95%); (f) NaOH, EtOH (90%); (g) ClCOCH₂COOEt, Et₃N, CH₂Cl₂ (100%); (h) NaOH, EtOH (96%); (i) BOP, NMM, DMF, HN-R³R⁴ (85–99%).

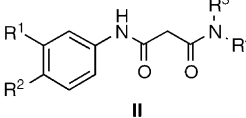


Scheme 2. Reagents and conditions: (a) Me-TosMIC, K₂CO₃, MeOH, reflux (79%); (b) 40 psi H₂, Pd/C, EtOH, (95%); (c) HOAc, Ac₂O, concd H₂SO₄, CrO₃, 0–10 °C (28%); (d) concd HCl, dioxane, reflux (99%); (e) TosMIC, K₂CO₃, MeOH, reflux (95%); (f) SnCl₂·2H₂O, EtOH/EtOH, reflux (95%).

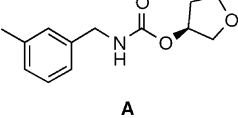
Table 1. SAR of diamides **I** and **II** for the inhibition of IMPDH II



I

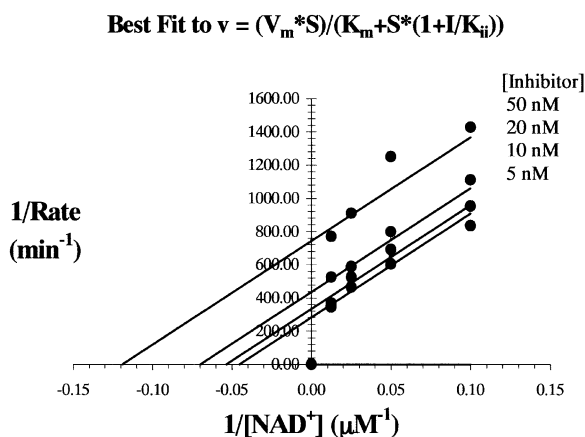


II



A

Compd	R ¹	R ²	R ³	R ⁴	IMPDH II IC ₅₀ , (μM)
Ia	OMe	5-Oxazolyl	H	Ph	0.052
Ib	OMe	5-Oxazolyl	Me	Ph	> 10
Ic	OMe	5-Oxazolyl	H	A	0.030
Id	OMe	5-Oxazolyl	H	NHPh	> 10
Ie	OMe	5-Oxazolyl	H	CH ₂ Ph	> 10
If	OMe	5-Oxazolyl	H	Cyclohexyl	> 10
Ig	OMe	5-Oxazolyl	H	<i>n</i> -Propyl	> 10
Ih	OMe	5-Oxazolyl	H	<i>iso</i> -Propyl	> 10
Ii	OMe	5-Oxazolyl	H	<i>t</i> -Butyl	0.010
Ij	OMe	5-Oxazolyl	Me	<i>t</i> -Butyl	> 10
Ik	OMe	5-Oxazolyl	H	C(Me) ₂ CH ₂ OH	0.019
Il	OMe	5-Oxazolyl	H	1-CH ₂ OH-Cyclopentyl	0.018
Im	OMe	5-Oxazolyl	H	C(Me) ₂ CO ₂ Me	0.074
In	OMe	5-Oxazolyl	H	C(Me) ₂ CH ₂ N(Me) ₂	0.047
Io	OMe	5-Oxazolyl	H	C(Me) ₂ CO ₂ H	> 10
Ip	OMe	5-Oxazolyl	H	C(Me) ₂ Ph	0.030
Iq	H	5-Oxazolyl	H	<i>t</i> -Butyl	> 10
Ir	H	4-Me-5-Oxazolyl	H	<i>t</i> -Butyl	> 10
Is	Br	5-Oxazolyl	H	<i>t</i> -Butyl	0.050
It	Cl	5-Oxazolyl	H	<i>t</i> -Butyl	0.055
IIa	OMe	5-Oxazolyl	H	Ph	0.40
IIb	OMe	5-Oxazolyl	H	<i>m</i> -Me-Ph	0.44

**Figure 2.** Uncompetitive inhibition of **II** versus NAD⁺ (see ref 14 for details).

IMPDH II. Substitution of the phenyl moiety at the meta position, which gives **IIb**, produced similar results. MPA is a potent inhibitor of mammalian IMPDHs ($K_i = 10$ nM for IMPDH II) and displays uncompetitive kinetics with respect to both IMP and NAD⁺. Likewise, VX-497 displays similar kinetics of inhibition. Compound **II** was found to be an uncompetitive inhibitor of with a $K_{ii} = 23 \pm 3$ nM (see Fig. 2).¹⁴ Due to the structural similarity to VX-497, this was not unexpected.

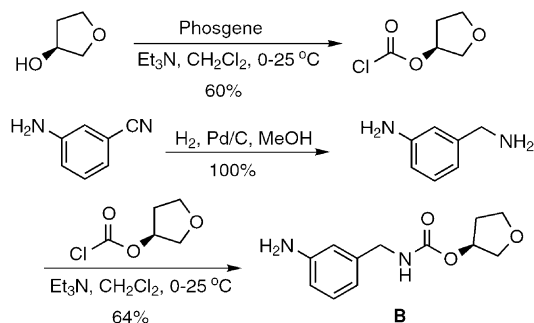
We have identified two new series of novel diamide-based inhibitors of IMPDH II catalytic activity. Compound **II**, a member of the ethanediamide structural class, is an uncompetitive inhibitor of IMPDH II with respect to NAD⁺ with a $K_{ii} = 23 \pm 3$ nM. Studies to

optimize this series of analogues to achieve oral activity in a B- and T-cell mediated pharmacodynamic model will be reported in due course.

References and Notes

- Jackson, R. C.; Weber, G. *Nature* **1975**, 256, 331.
- Collart, F. R.; Huberman, E. *J. Biol. Chem.* **1988**, 263, 15769.
- Natsumeda, Y.; Ohno, S.; Kawasaki, H.; Konno, Y.; Weber, G.; Suzuki, K. *J. Biol. Chem.* **1990**, 265, 5292.
- Collart, F. R.; Huberman, E. US Patent 5,665,583, 1997; *Chem. Abstr.* **1997**, 113, 186070.
- Anderson, W. K.; Boehm, T. L.; Makara, G. M.; Swann, R. T. *J. Med. Chem.* **1996**, 39, 46.
- Nelson, P. H.; Eugui, E.; Wang, C. C.; Allison, A. C. *J. Med. Chem.* **1990**, 33, 833.
- Sievers, T. M.; Rossi, S. J.; Ghobrial, R. M.; Arriola, E.; Nishimura, P.; Kawano, M. *Holt Pharmacother.* **1997**, 17, 1178.
- Markland, W.; McQuaid, T. J.; Jain, J.; Kwong, A. D. *Antimicrob. Agents Chemother.* **2000**, 44, 859.
- Sintchak, M. D.; Nimmesgern, E. *Immunopharmacology* **2000**, 47, 163.
- Armistead, D. M.; Badia, M. C.; Bemis, G. W.; Bethiel, R. S.; Frank, C. A.; Novak, P. M.; Ronkin, S. M.; Saunders, J. O. PCT Int. Appl., WO 9740028, 1997; *Chem. Abstr.* **1997**, 128, 3680.
- BOP reagent: benzotriazol-1-yloxy-tris(dimethyl-amino)-phosphonium hexafluoro-phosphate.
- Possel, O.; van Leusen, A. M. *Tetrahedron Lett.* **1997**, 48, 4229.
- Gu, H. H.; Dhar, T. G. M.; Iwanowicz, E. J. PCT Int. Appl., WO 0026197, 2000; *Chem. Abstr.* **2000**, 132, 334449.

Scheme for the synthesis of **B**:



14. The enzymatic activity of human IMPDH II was quantitated using a procedure similar to reported methods.^{15,16} The conversion of NAD^+ to NADH was followed spectrophotometrically at 340 nm [$\epsilon = 6220 \text{ M}^{-1} \text{ cm}^{-1}$]. Quartz cuvettes (1.0 cm path length) were used, with a total volume of 1.00 mL. The assay buffer consisted of 50 mM Tris, pH 8.0, 100 mM KCl, 2 mM EDTA, 3 mM DTT, 1.00 mM IMP, and

variable concentrations of NAD^+ (10, 20, 40, and 80 μM ; $K_m = 27 \mu\text{M}$). The protein concentration used for K_i determinations was 10 nM, and reactions were initiated by adding enzyme. A solution of inhibitor was prepared in DMSO (20 mM), and diluted serially. Four concentrations of **II** were used to calculate K_i (5, 10, 20, and 50 nM), maintaining a final volume of 2.5% v/v DMSO. Samples were analyzed using a Cary Model 3E Uv-vis spectrophotometer equipped with a Peltier temperature controller maintained at 37 °C. Software provided by the instrument manufacturer was used to calculate the initial rates of reaction as the linear least-squares fit to each data set. To determine the K_i value, the initial velocity data (rate per min) were fitted globally using the competitive, uncompetitive, and non-competitive models with KinetAsyst kinetics software (IntelliKinetics, Princeton, NJ, USA). The best fits were obtained to the uncompetitive model of inhibition for **II**, and shown above in Figure 1. Note the point at the origin is an artifact of the fitting program.

15. Carr, S. F.; Papp, E.; Wu, J. C.; Natsumeda, Y. *J. Biol. Chem.* **1993**, 268, 27286.

16. Xiang, B.; Yalor, J. C.; Markham, G. D. *J. Biol. Chem.* **1996**, 271, 1435.